

A deformable surface model with volume preserving springs

Arnab, S. and Raja, V.

Author post-print (accepted) deposited in CURVE August 2013

Original citation & hyperlink:

Arnab, S. and Raja, V. (2008). A deformable surface model with volume preserving springs. In F.J. Perales and R.B. Fisher (Eds). *Proceedings of the 5th International Conference on Articulated Motion and Deformable Objects* (pp. 259-268). New York: Springer.

http://dx.doi.org/10.1007/978-3-540-70517-8_25

Publisher statement: The final publication is available at <http://link.springer.com/>.

Copyright © and Moral Rights are retained by the author(s) and/ or other copyright owners. A copy can be downloaded for personal non-commercial research or study, without prior permission or charge. This item cannot be reproduced or quoted extensively from without first obtaining permission in writing from the copyright holder(s). The content must not be changed in any way or sold commercially in any format or medium without the formal permission of the copyright holders.

This document is the author's post-print version of the journal article, incorporating any revisions agreed during the peer-review process. Some differences between the published version and this version may remain and you are advised to consult the published version if you wish to cite from it.

CURVE is the Institutional Repository for Coventry University

<http://curve.coventry.ac.uk/open>

A Deformable Surface Model with Volume Preserving Springs

Sylvester Arnab, Vinesh Raja

University of Warwick
CV4 7AL, Coventry, UK
E-mail: s.arnab@warwick.ac.uk

Abstract. This paper discusses the possibility of employing a surface model to emulate volume behaviour. This is inspired by a significant interest in employing the surface data due to its simplicity. However, there are issues in properties estimation and volume preservation. Therefore, the aim of the ongoing research includes exploring the potential of a surface mass spring model with shape-preserving springs for volume simulation. Initial evaluations illustrate the feasibility of employing a mass spring model with volume preserving springs to simulate the dynamic behaviour of a soft volume. The proposed framework can be further explored to address other material properties.

Keywords: Deformable Model, Mass Spring Systems, Volume Preservation

1 Introduction

The dynamic behaviour of human organs can be replicated using the soft solid simulation techniques. These organs are initially modelled into 3 dimensional volumes based on medical data such as CT/MRI scans. This volume data can then be rendered in a virtual environment based on the organ's material and mechanical properties. The haptic devices provide the tactile interaction with the model in the virtual environment, which makes it more useful in areas such as the medical training.

However, due to the benefit of having a less complex mesh network, surface data is increasingly being utilised to emulate volumetric solid behaviour. The main issue is constant volume preservation as well as correct volume behaviour during simulation. Generally, a surface model would collapse under gravity and without the internal volume, determining the correct deformation effect would be a challenge.

2 Related Works

Commonly, surface data is re-meshed in order to create internal volume. However, this creates computational overhead during simulation imposed by a more complex

volume network. The addition of new artificial springs [1] to the existing volume mesh produces a stiffer object [2]. [3] [4] addressed shape preservation and [2] introduced weighted constraints that control the deformation distribution of the muscle instead of using additional springs. However, this method is fundamentally focusing on the local radius of influence of the interaction and is not influenced by the orientation of the interaction force.

A more effective shape preserving method has been embedded into the Mass Spring Systems (MSS) where springs are placed at the nodes. They are also known as the Local Shape Memory [5]. These springs have been employed to simulate non-linear skin behaviour of a virtual thigh [6] [7]. [8] administered these springs to preserve object shape during simulation. However, the stiffness of the springs was either statistically fine-tuned based on predefined properties [9] or regularly distributed. [10] extended this method by extracting the properties of the springs based on radial links [11][12].

Volume behaviour is influenced by the properties estimated for the model. Regular properties distribution is very common where the regular node concentration is assumed [1] [13] [14] [15]. In the case of irregular node concentrations, the mesh topology is modified to be as regular as possible [16] [17]. However, when a portion of the surface model is refined, the regular topology becomes irregular. Consequently, the properties require re-estimation within the refined area. [8] attempted properties re-estimation after surface refinement but the behaviour patterns between the coarse and the refined area do not coincide. The behaviour has been improved by our method discussed in [10] where these patterns achieve a higher level of co-incidence.

3 The Proposed Deformable Model

The scope of dynamic behaviour in this research is within a constrained space such as a human breast fixed on a static body (Fig. 1). The model is constructed from the surface mesh and the dynamic behaviour is achieved by employing the surface MSS with volume preserving springs.

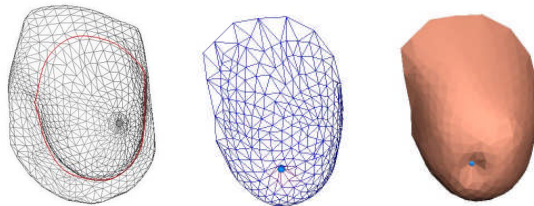


Fig. 1. A breast model (geometrical mesh and rendered model)

To address the issue of properties estimation as well as the non-existence of inner volume for the proposed surface model, the object's internal volume represented by the surface elements has to be considered. This framework extended the scheme

described in [10], where a surface mass spring systems with additional shape preserving springs are employed.

3.1 Surface Mass Spring Systems (SMSS)

The SMSS is based on the surface mesh topology where the springs are represented by the edges of the triangular elements (Fig. 2). For instance, the edge that connects the nodes with mass m_i and m_j is the spring with stiffness k_{ij} .

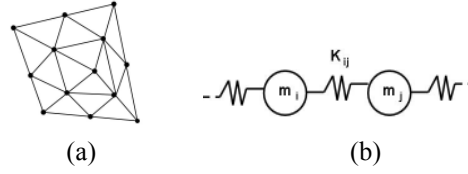


Fig. 2. a) Nodes connected by edges (b) A pair of nodes connected by a spring

For the spring link ij , the internal force F_{ij} is

$$F_{ij} = K_{ij} \left(\|p_j - p_i\| - l_{ij} \right) \frac{p_j - p_i}{\|p_j - p_i\|} \quad (1)$$

, where $\|p_j - p_i\|$ is the magnitude of the displacement of the current state of the spring link ij , l_{ij} is the rest length of the spring link, and K_{ij} is the stiffness (spring) coefficient of the node pair. The spring stiffness is estimated based on a distribution algorithm described in [10] [13] [18] [19].

3.2 Volume Preserving Springs

The proposed volume springs (Fig. 3) are commonly utilised to preserve the shape of the model at equilibrium. They behave in a similar way as the surface spring but the rest length of each spring is zero.

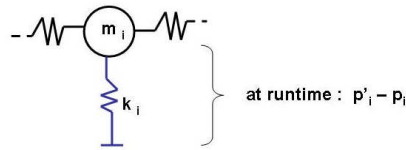


Fig. 3. The inner spring that provides a volumetric support to the mass at i

Based on Equation (1), the reaction force imposed on the mass at node i ,

$$F_i = K_i \left(\|p'_i - p_i\| \right) \frac{p'_i - p_i}{\|p'_i - p_i\|} \quad (2)$$

, where K_i is the stiffness of the inner spring at node i , p'_i is the new position of node i at runtime and p_i is the anchored position of node i . In order to not only preserve the object shape but also maintain a constant volume during simulation, the concept of these shape preserving springs has been extended.

3.3 Volume Discretisation for Properties Estimation

The relationship between the deformable model and the real material is important. The elasticity modulus of a material is extracted from the stress and strain relationship, where a constant magnitude of force is imposed along the axis parallel to the normal of the surface. The initial volume discretisation supported by each node should support this relationship. In a MSS, force directly influences the dynamic behaviour of the nodes. Therefore, the volume supported by a node should be discretised along its normal.

The radial link method in [10] is extended, where the new distance vector with length L'_i , relative to the object centre of mass, the initial length L_i and the surface normal at the node, are derived. The new volume (Fig. 4) is based on node i relative to the new centre point c_i and the other nodes or vertices of the triangular element. The new L'_i is the scalar projection of L_i along the normal unit vector of point i . This explicit method guides the estimation of mass and spring stiffness for all nodes relative to their respective normals and neighbouring triangles.

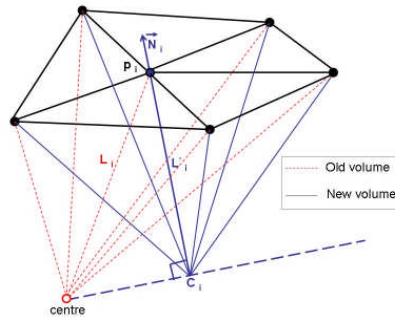


Fig. 4. Volume discretisation relative to the normal at node i

3.4 Properties Estimation

Based on the discretisation (Fig. 4), mass at node i is estimated as

$$m_i = \frac{\sum_{i \in I} V_i}{\sum_{j=0} V_j} M$$

, where the estimation ratio for each node is the total volume under the neighbouring triangular elements t (of which node i is a member) divided by the total volume for all n nodes, and M is the object mass.

The stiffness of the volume preserving springs describes the level of elasticity of the virtual space or volume represented by the node. Therefore, the value of the stiffness is influenced by the stress and strain relationship along the axis parallel to the normal at the node. The stiffness dimension based on Young's Modulus and shear modulus is initialised before the simulation. The dimension is defined as

$$\begin{bmatrix} K_E \\ K_G \end{bmatrix}_i = E \sum_{t \in t} \frac{V_t}{L_i^2} \begin{bmatrix} 1 \\ 1/2(1-\nu) \end{bmatrix}$$

, where K_E and K_G are the spring stiffness based on linear elasticity modulus and shear (rigidity) modulus respectively, E is the Young's Modulus and ν is the Poisson Ratio of the material.

The behaviour of the spring stiffness at runtime depends on the orientation of the acting force along each spring. The stiffness K_i of the spring at each node i can be determined at runtime:

$$K_i = \begin{bmatrix} \|\vec{N}_i \cdot \vec{F}_i\| & 1 - \|\vec{N}_i \cdot \vec{F}_i\| \end{bmatrix} \begin{bmatrix} K_E \\ K_G \end{bmatrix}_i$$

, where N and F are the normal and force at node i .

3.5 Volume Preservation

In order to preserve volume during simulation, the spring dimension can be extended to address other properties such as bulk elasticity as a factor against volume variation during simulation. Bulk stiffness K_B at node i is

$$K_{Bi} = \frac{E}{3(1-2\nu)} \sum_{t \in t} \frac{V_t}{L_i^2}$$

Volume displacement during simulation can be derived based on the volume calculation employed in [2]. This calculation will be correct even when the surface becomes concave during simulation. Therefore, force at node i along its normal unit vector at a time step without any external force interaction on the surface is

$$F_i = K_{Bi} \Delta V w_i \vec{N}_i \quad (3)$$

, where ΔV is the volume displacement, and w_i is the constraint that controls the distribution of the volume penalty force. The constraint is set to 1, which means volume change affects all nodes equally but constrained by their respective bulk stiffness. Therefore, in order to correctly distribute the interaction force effect to the object surface, the constraint is estimated based on the interaction radius of influence

where, the sum of the constraints is equal to the number of nodes. The radius of influence [2] has been modified and the interaction force orientation is introduced as the correction factor. If the surface nodes are within the radius of influence r , weight at node i is

$$w_i = \left(\frac{\mathbf{p}_i - \mathbf{p}_f}{\|\mathbf{p}_i - \mathbf{p}_f\|} \cdot \vec{F}_f \right) \left(\cos \left(\frac{\|\mathbf{p}_i - \mathbf{p}_f\|}{r * 2} * \Pi \right) \right) \quad (4)$$

, where \mathbf{p}_i and \mathbf{p}_f are the position vector of node i and the position of where force is imposed respectively. Since the sum of weighted constraints is equal to the number of nodes [2], the constraint values have to be normalised. Therefore, based on Equation (3) and (4), the penalty force at node i is

$$F_i = K_s \Delta V w_i \frac{\mathbf{p}_i - \mathbf{p}_f}{\|\mathbf{p}_i - \mathbf{p}_f\|}$$

4 Empirical Experiments

The framework for the experiments has been implemented on top of Microsoft Visual C++, OpenGL and OpenHaptics platforms. Phantom Desktop haptic device enables interaction and the desktop PC has the specification of Intel Pentium 4, 2.40 GHz and 1 G RAM. Each time step denotes 0.01 s. To evaluate the estimation method and the feasibility of having a 3 dimensional stiffness, 2 schemes have been compared:

- **Scheme A** : Irregular mass and inner stiffness (single stiffness dimension)
- **Scheme B** : The Proposed Estimation

Further comparisons are carried out against the Finite Element Model (FEM) and volume MSS (VMSS). The elasticity modulus is re-extracted from the model to evaluate if the proposed model emulates the same material behaviour.

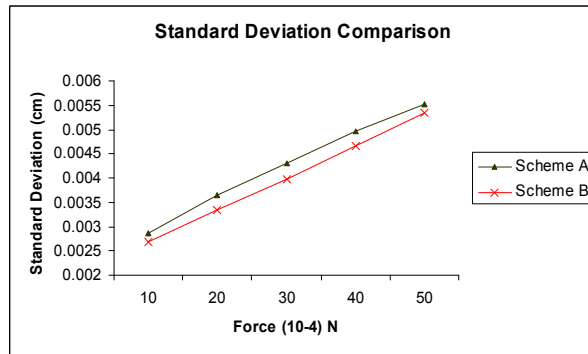
4.1 Properties Estimation

To evaluate properties estimation, a local area is refined and the properties are then re-estimated. A constant force is imposed on a node and the displacement data is collected. The displacement patterns within the coarse and the refined area are compared. If the patterns are identical, the deformation behaviour is preserved despite the change in the mesh topology. The displacement behaviours are studied where 2 values are analysed:

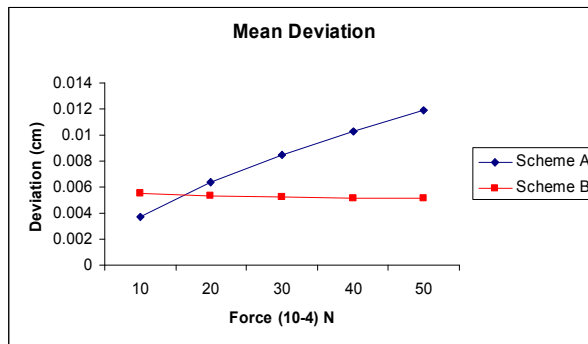
- i) The standard deviation between the 2 patterns determines their level of co-incidence. The smaller the standard deviation, the more identical the patterns are

- ii) The mean deviation of the 2 patterns represents the error in behaviour after refinement. The least value indicates the least deviation from the original behaviour

Fig. 5 describes the findings based on a sphere model with irregular mesh topology to illustrate the concept. The standard deviations comparison in 5(a) shows that B produces high level of co-incidence between the patterns. Furthermore, it maintains a minimal displacement deviation for any magnitude of force compared to A which deviation increases with force (5(b)). Hence, the analysis concludes that B preserves the properties and behaviour with minimal standard deviation when a local area is refined. Tests have been carried out on models with various mesh complexities and they also draw similar conclusions.



(a)



(b)

Fig. 5. (a) The standard deviation (b) Average displacement deviation

The stiffness of the springs is based on the real elasticity properties of the material. Therefore, to evaluate scheme B, the Young's modulus (E) can be derived from the strain and stress relationship of the deformable model and compared to the original E. The values (Table 1) demonstrate that the deformable surface model can closely emulate the volume material behaviour.

Table 1. The Young's Modulus (E) extracted from the model when a constant stretching force is imposed on the surface of a cube.

Model (nodes)	Cube (602)	Cube (1352)	Cube (2402)
E (67 Pascal)	67.80	66.80	67.00
E (100 Pascal)	100.07	98.70	98.70
E (3.25 Kpa)	3.30	3.17	3.11

4.2 Performance

A simple performance test has been carried out to illustrate that the surface data reduces the computational cost. Table 2 shows that the average frame per second (FPS) achieved by the VMSS and the proposed surface model.

Table 2. Total FPS Comparison

Model (number of surface nodes)	Cube (602)	Cube (1352)	Cube (2402)	Sphere (1000)
VMSS	77	37	20	47
Scheme B	80	44	25	77

4.3 Volume Behaviour

To produce a more realistic global deformation based on the interaction force radius and orientation of influence, the weighted constraint is manipulated at runtime.

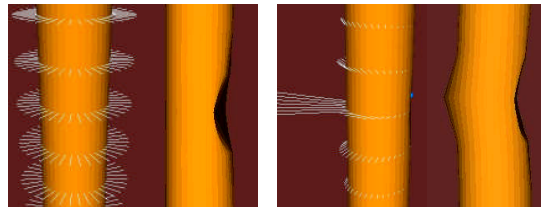


Fig. 6. (a) Constraints are uniform (b) Constraints extracted at runtime

When the constraints are set to 1, the global deformation as in Fig. 6 (a) is produced. Upon interaction, the constraint at each node is updated in regards to the radius and the interaction force orientation. Consequently, figure 6 (b) shows that the automatic constraint derivation produces a more realistic behaviour.

Other models such as cubes with different surface mesh complexities have been compared with the FEM model as analysed by SolidWorks/Cosmos. A shear force is imposed on the top surface while the opposite surface is fixed. When compared with FEM, the shape produced is similar with minor deviation (Fig. 7).

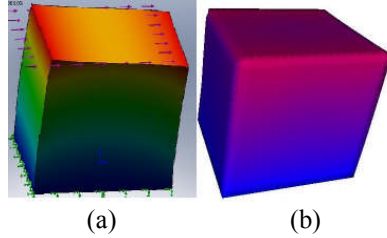


Fig. 7. Shape comparison (a) FEM (b) Scheme B

When a constant force is imposed on the surface, the object shape changes and deforms. The analysis concludes that scheme B preserves the object volume with the least volume deviation as illustrated in Fig. 8.

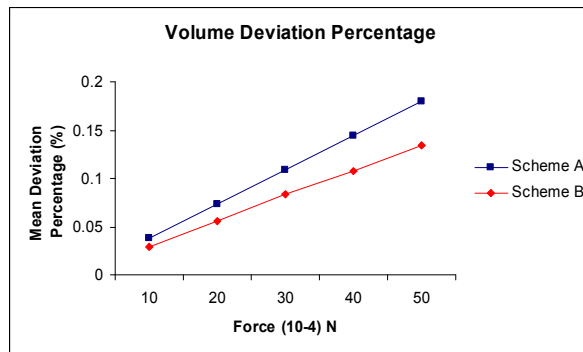


Fig. 8. The percentage of the average volume deviation

Conclusions

This paper has illustrated the feasibility of employing a surface mesh to simulate soft volume. The proposed framework introduces volumetric discretisation based on the node normal, the anisotropic extraction of inner spring relative to force orientation as well as weighted constraints to control global deformation effect. Local deformation behaviour is preserved regardless of the mesh resolutions and global deformation effect is achieved despite the non-existence of internal volume. It displays similar behaviour with the FEM model and produces minimal deviation from the original elasticity modulus. Furthermore, the computational performance is better than the volume counterpart. Even though the proposed method is based on materials that are linearly elastic, homogeneous and incompressible, it can also be extended to address other properties.

The framework is currently explored in the ongoing research in breast simulation. Further evaluations such as the perception test with the users will be carried out to verify the visual and haptic feedback experienced by the users

References

1. Bourguignon D. and Cani M. P.: Controlling Anisotropy in Mass-Spring Systems, Computer. *Animation and Simulation 2000*, 113-123
2. Hong M., Jung S., Choi M., Welch S.: Fast Volume Preservation for a Mass-Spring System, *IEEE Computer Graphics and Applications*, September/October 2006, 83-91
3. Nedel L. P. and Thalmann D.: Real-Time Muscle Deformations Using Mass Spring Systems, Proc. Computer Graphics Int'l, IEEE Press, 1998, pages 156-165
4. Aubel A, Thalmann D: Realistic Deformation of Human Body Shapes, Proc. Computer Animation and Simulation 2000, Interlaken, August 2000, pp. 125-135.
5. Marchal M., Promayon E.: Troccaz J.: Simulating Complex Organ Interactions: Evaluation of a Soft Tissue Discrete Model, ISVC 2005, LNCS 3804, pages 175-182, © Springer-Verlag Berlin Heidelberg 2005
6. Mendoza C., Sundaraj K.; Laugier C.: Issues in Deformable Virtual Objects Simulation with Force Feedback, *International Advanced Robotics Program (IARP): International Workshop on Human Robot Interfaces*, Rome - Italy, 2002.
7. Laugier C., Mendoza C., Sundaraj K: Towards a Realistic Medical Simulator using Virtual Environments and Haptic Interaction, Robotics Research: The Tenth International Symposium, Springer Tracts in Advanced Robotics Volume 6/2003
8. Choi Y., Hong M., Choi M.; Kim M.: Adaptive Surface-deformable Model with Shape-preserving Spring, *Journals of Computer Animation and Virtual Worlds*, Comp. Anim. Virtual Worlds 2005, number 16, pages 69-83
9. Zhang J., Payandeh S., Dill J.: Haptic Subdivision: an Approach to Defining Level-of-Detail in Haptic Rendering, Proceedings of the 10 Symposium on Haptic Interfaces for Virtual Environment and Teleoperator Systems, Orlando, FL, March, 2002, pages 201-208
10. Arnab S., Raja V.: Irregular *Surface Mesh Topology for Volumetric Deformable Model*, The 4th INTUITION International Conference and Workshop, 4-5 October 2007, Athens, Greece
11. Vassilev T. and Spanlang B.: A Mass-Spring Model for Real Time Deformable Solids, Proceedings of East-West Vision 2002, pp. 149-154, Graz, Austria, September 12-13, 2002
12. Balaniuk R. and Salisbury K.: Soft Tissue Simulation using the Radial Element Method, IS4TM-International Symposium on Surgery Simulation and Soft Tissue Modelling, France, June 12-13 2003
13. Gelder A. V.: Approximate Simulation of Elastic Membranes by Triangulated Spring Meshes, *Journal of Graphics Tools* 1998, 3(2), pages 21-41
14. Delingette H.: Towards Realistic Soft Tissue Modeling in Medical Simulation, *Proceedings of the IEEE: Special Issue on Surgery Simulation*, 512-523, April 1998
15. Brown J., Sorkin S., Bruyns C.: Real Time Simulation of Deformable Objects: Tools and Application, *In Comp. Animation*, 2001
16. Deussen O., Kobbelt., Tucke P.: Using Simulated Annealing to Obtain Good Nodal Approximations of Deformable Objects, *Computer Animation and Simulation '95*, Springer-Verlag, 1995
17. Bielser D.: A Framework for Open Surgery Simulation, *Doctor of Technical Sciences Thesis*, Swiss Federal Institute of Technology, ETH, Zurich, 2003
18. Maciel A., Boulic R., Thalmann D.: Towards a Parameterization Method for Virtual Soft Tissues Based on Properties of Biological Tissue, In International Symposium on Surgery Simulation and Soft Tissue Modeling, 2003
19. Lloyd B. A., Szekely G., Harders M.: Identification of Spring parameters for Deformable Object Simulation, *IEEE Transactions on Visualisation and Computer Graphics*, Vol. 13, No. 5, Sept/Oct 2007